



Optimization of Heat Recovery for Shell & Tube Exchangers in Sulphur Granulation Unit of South Pars Fifth Refinery by Software, ASPEN B-JAC

Kazem Moaveni*, Mehran Zarkesh

Department of Mechanic, Dashtestan Branch, Islamic Azad University, Borazjan, Iran

Email address:

kazemmoaveni@gmail.com (K. Moaveni)

*Corresponding author

To cite this article:

Kazem Moaveni, Mehran Zarkesh. Optimization of Heat Recovery for Shell & Tube Exchangers in Sulphur Granulation Unit of South Pars Fifth Refinery by Software, ASPEN B-JAC. *American Journal of Mechanical and Industrial Engineering*. Vol. 2, No. 4, 2017, pp. 162-173. doi: 10.11648/j.ajmie.20170204.12

Received: April 28, 2017; **Accepted:** May 6, 2017; **Published:** July 5, 2017

Abstract: Shell and tube heat exchangers are the most important tools in heat transfer process. Optimization efficiency of these tools is always the goal of designers. Now a day there are a lot of efficient methods for selecting the best heat exchanger, such as analytic and numerical methods that everyone has advantages and defects. For example, confront of jamming in calculations by receiving to the local minimums and errors during interruption quantities. Today by entering of simulation and design softwares in industries, the simulation of process tools is so simple. the procedure of studies in this thesis is in these steps: first simulation of sulfur solidification heat exchangers in ASPEN B-JAC software same as operation conditions and then evaluation the effects of changing the design parameters in tube bundle section such as number of passes, arrangement of tubes, number of baffles,.... the sulfur solidification package' heat exchanger that it's active fluid is demine water for cooling of package will be optimized till the rate of exchanged heat increases to 15 percent and pressure drop will not affect the operation conditions. The most important note in the correction of tube bundle is that the heat exchanger should be out of service and stopping of production, on the other hand changing in shell of heat exchanger needs to change the piping system and redesign of supports that will spend a lot of time for shut down of plant, so it is out of order for this thesis and optimization of tube bundle will be done.

Keywords: Optimization, Heat Recovery, Shell and Tube Exchanger, Sulphur Granulation, ASPEN B-JAC

1. Introduction

Natural gas is the most important source of energy with characteristics such as cleanliness and cheapness that make it more important. Increasing speed in converting gas to the fuel consumption in petrochemical industry, transportation industry and most importantly the cost of urban gas has made it one of the most important determining factor in the country's energy. The effectiveness and efficiency of refinery units is therefore of great importance to increase production. The aim of this study is to assess the possibility of reducing energy consumption in the South Pars gas refineries.

2. The Governing Equations for the Design of Shell and Tube Exchanger

2.1. Calculated the Hrat Transfer and Pressure Drop in Shell Side by KERN

2.1.1. The Coefficient of Heat Transfer at the Shell Side

The coefficient of heat transfer at the outer of the tubes bundle called The coefficient of heat transfer in shell side and The coefficient of heat transfer calculate based on the diameter D_e .

KERN suggested the following equation for calculate of heat transfer coefficient in the shell side:

$$\frac{h_0 D_e}{k} = 0.36 \left(\frac{D_e G_s}{\mu} \right)^{0.55} \left(\frac{c_p \mu}{k} \right)^{\frac{1}{3}} \left(\frac{\mu_b}{\mu_w} \right)^{0.14} \quad (1)$$

for

$$2 \times 10^3 < Re_s = \frac{G_s D_e}{\mu} < 1 \times 10^6 \quad (2)$$

Where in h_0 is heat transfer coefficient in the shell side and D_e is the diameter of the shell and G_s is mass speed of shell side.

The diameter of the shell is quadruple the pure surface of flow divided by the wetted perimeter that the pure surface of flow determined by tube locating on tube sheet (for locating with square pitches and or triangular pitches).

$$D_e = \frac{4 \times \text{surface area of free flow}}{\text{the wetted perimeter}} \quad (3)$$

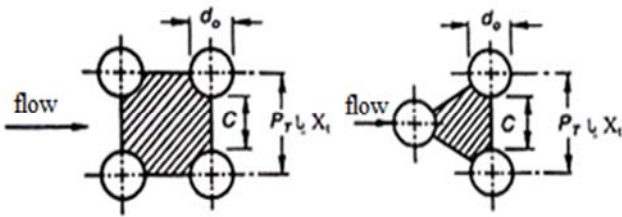


Figure 1. Locating of square pitch and triangular pitch of tube.

So, for square pitch, can be written:

$$D_e = \frac{4 \left(P_T^2 - \frac{\pi d_o^2}{4} \right)}{\pi d_o} \quad (4)$$

And for triangular pitch:

$$D_e = \frac{4 \left(\frac{P_T^2 \sqrt{3}}{4} - \frac{\pi d_o^2}{8} \right)}{\frac{\pi d_o}{2}} \quad (5)$$

In shell side, there is no free flow area which calculate mass speed in the shell side G_s in this reason amounts G_s can to be defined based on the level maximum of the hypothetical flow, that the distance between the tubes making in a row, in the diameter of the shell.

Variable that affect on the speed are shell diameter D_s , clearance C between neighbor tubes, the pitch size P_T and partition distance B . width of flow level is in the rows of set tubes in shell center $(D_s/P_T)XC$ and considered to be the length of flow level of wall distance B .

So, cross flow surface area with tube bundle, in the shell center A_s is:

$$A_s = \frac{D_s}{P_T} (C). B \quad (6)$$

Where in D_s is the inner diameter of the shell. so, flow mass speed in shell side is obtained the from following equation:

$$G_s = \frac{\dot{m}}{A_s} \quad (7)$$

2.1.2. Pressure Drop at the Shell Side

Pressure drop at the shell side depends to number of tubes,

times number of flow crossing from tube bundle between walls and the length each intersection. if suppose that divided the tube bundle length with 4 walls, as a result all fluid, 5 times will be in width of tube bundle with that the intersection.

By multiplying the distance in along vertical sheet on tube bundle, that can considered it to the inner diameter of the shell D_s and number of times that flow cuts tube bundle, relationship is obtained for calculate of pressure drop in tube side.

The diameter for calculate of pressure drop is like The diameter for heat transfer. Pressure drop at the shell side is calculated with the following expression.

$$\Delta P_s = \frac{f G_s^2 (N_b + 1) D_s}{2 \rho D_e \phi_s} \quad (8)$$

That $\phi_s = (\mu_b / \mu_w)^{0.14}$, N_b is number of walls and $(N_b + 1)$ is times number that flow in the shell, cut the tube bundle. the friction coefficient f calculate for shell from the following equation:

$$f = \exp(0.576 - 0.19 \ln Re_s) \quad (9)$$

Where in:

$$400 < Re_s = \frac{G_s D_e}{\mu} \leq 1 \times 10^6 \quad (10)$$

The gained friction coefficient is included, losses of flow entrance to shell and losses of flow output from the shell.

2.1.3. Pressure Drop at the Tube Side

Pressure drop in tube side, with having, number of tube passes N_p and the length of heat exchanger L is calculated.

Pressure drop for flow of tube side is calculated by the the following equation:

$$\Delta P_r = 4 N_p \frac{\rho U_m^2}{2} \quad (11)$$

or

$$\Delta P_t = 4 f \frac{L N_p}{d_i} \frac{G_t^2}{2 \rho} \quad (12)$$

Changing direction in tube passes creates additional Pressure drop Δp_r that is due sudden expansion and contraction that crossing fluid from tube will be during the back and needed for the per-pass tube be considered 4 times speed head.

So, total pressure drop in tube side is:

$$\Delta P_{\text{total}} = \left(4 f \frac{L N_p}{d_i} + 4 N_p \right) \frac{\rho U_m^2}{2} \quad (13)$$

2.2. Bell - Delaware Method

Analysis at the shell side is not as simple as analysis at tube side. The reason is that flow in the shell is complicated and the form is a combination of Cross flow, flow in the window of walls, by pass flow of the wall, and the flow in the shell and tube. This complicated pattern of flow is shown

in figures 1 and 2.

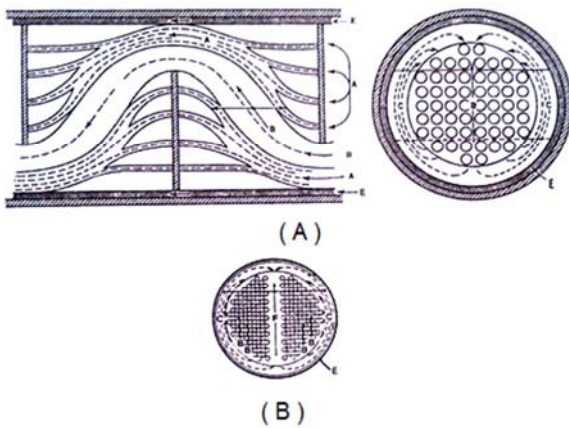


Figure 2. A) The diagram shows leakage paths for bypass flows of tube matrix including clearance leakages between walls, and shell and also flow between tube matrix and shell B) F flow for exchanging heat with two tube pass.

As shown in figure 1, 5 different flows are recognized. Flow A is the leakage in looseness between tubes and wall. Flow B is the cross main flow with the tube bundle. This favorable flow is at the shell side of heat exchanger. Flow C is the bypass flow of the tube bundle that is in flow in among the tube bundle between tubes outermost in the tube bundle and inner surface of the shell. Flow E is the leakage flow between the wall and shell that is in flow in the looseness between wall and the inner diameter of the shell.

Then there is flow F, that is current in every channel and used for making several tube pass in tube bundle lead. The above figure is an ideal figure of the above mentioned flows. The shown flows can be mixed and affect each other. A more completed mathematical analysis of the flow at shell side can take these issues into account.

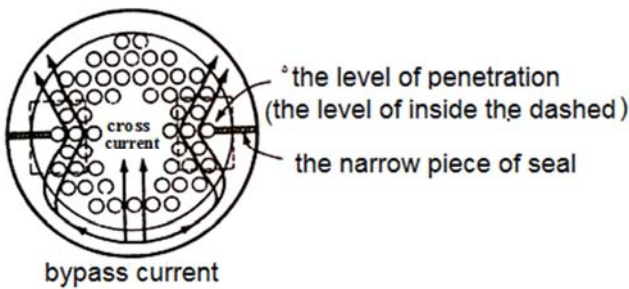


Figure 3. Design radial walls for decrease of bypass flow from looseness between shell and tube matrix.

A brief discussion is provided in this section that is about Bell - Delaware's method for analyzing the pressure drop and the coefficient for the heat transfer at the shell side.

2.2.1. The Coefficient of Heat Transfer at the Shell Side

The basic equation for the average calculating of coefficient of heat transfer at shell side is shown with the following relation

$$h_o = h_{id} J_\ell J_b J_s J_r \tag{14}$$

in which h_{id} is the ideal of The coefficient of heat transfer for fully cross-flow with ideal tube bundle and is shown with the following relation:

$$h_{id} = j_{id} c_{Ps} \left(\frac{\dot{m}}{A_s}\right) \left(\frac{k_s}{c_{Ps}\mu_s}\right)^{\frac{2}{3}} \left(\frac{\mu_s}{\mu_{s-w}}\right)^{0.14} \tag{15}$$

In which j_{id} is the coefficient of j_{id} related to Colburn for a set of ideal tube, S is representative of the shell, and A_s is the cross flow surface area with the tubes at the shell center line between the two walls.

There are charts for determining j_{id} as a function of Reynolds number at the shell side flow, $Re_s = d_o \dot{m}_s / \mu_s A_s$, there are tube placement, And the size of pitch. such charts are represented in figures 3 to 5.

As is calculated based on the equation 3

$$A_s = \frac{D_s}{P_T} (C). B \tag{16}$$

Reynolds number is calculated based on the outer tube diameter and the minimum area of flow surface in the shell diameter.

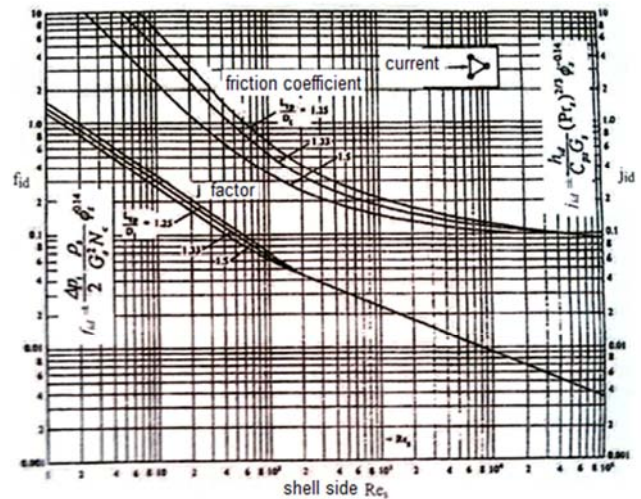


Figure 4. Coefficients of J_M and f_M , set of ideal tube for locating the periodic of 30 degree.

Although ideal amounts of j_{id} and f_{id} are provided in the form of a diagram, for calculations and analysis with the help of computer, the set of relations which are obtained from the above diagrams are employed in the following way:

$$j_{id} = a_1 \left(\frac{1.33}{P_T}\right)^a (Re_s)^{a_2} \tag{17}$$

in which

$$a = \frac{a_3}{1+0.14(Re_s)^{a_4}} \tag{18}$$

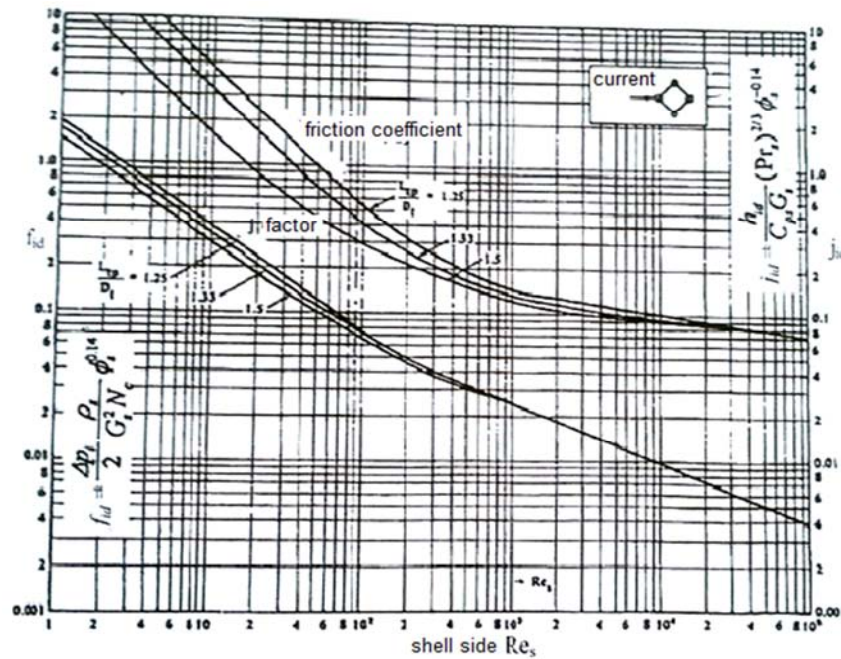


Figure 5. Coefficients of J_M and f_M , set of ideal tube for locating the periodic of 45 degree.

and pressure drop coefficient is:

$$f_{id} = b_1 \left(\frac{1.33}{\frac{P_T}{d_o}} \right)^b (Re_s)^{b_2} \tag{19}$$

in which

$$b = \frac{b_3}{1+0.14(Re_s)^{b_4}} \tag{20}$$

the coefficient of the relations 10 and 11 are provided in table 1.

Table 1. Empirical coefficients for J_i and F_i .

Locating angle	Reynolds number	a_1	a_2	a_3	a_4	b_1	b_2	b_3	b_4
30°	$10^5 - 10^4$	0.321	-0.388	1.450	0.519	0.372	-0.123	7.00	0.500
	$10^4 - 10^3$	0.321	-0.388			0.486	-0.152		
	$10^3 - 10^2$	0.593	-0.477			4.570	-0.476		
	$10^2 - 10$	1.360	-0.657			45.100	-0.973		
	< 10	1.400	-0.667			48.000	-1.000		
45°	$10^5 - 10^4$	0.370	-0.396	1.930	0.500	0.303	-0.126	6.59	0.520
	$10^4 - 10^3$	0.370	-0.396			0.303	-0.136		
	$10^3 - 10^2$	0.730	-0.500			3.500	-0.476		
	$10^2 - 10$	0.498	-0.656			26.200	-0.913		
	< 10	1.550	-0.667			32.00	-1.000		
90°	$10^5 - 10^4$	0.370	-0.395	1.187	0.370	0.391	-0.148	6.30	0.378
	$10^4 - 10^3$	0.107	-0.266			0.0815	+0.022		
	$10^3 - 10^2$	0.408	-0.460			6.0900	-0.602		
	$10^2 - 10$	0.900	-0.631			32.10000	-0.963		
	10	0.970	-0.667			35.0000	-1.000		

J_c is the correction coefficient for the percentage of partitions cutting and the distance between them. This coefficient of heat transfer at the window site (the area that is cut and separated) should be taken into account and the total heat transfer coefficient should be calculated for the whole heat exchanger. This coefficient is dependent on the shell inner diameter and the distance with the wall (cut height of partition). For a big cutting of the wall, this coefficient may

decrease up to 0.53 and for a heat exchanger without any tube at the window site, the amount of this coefficient is about 1. This coefficient may increase up to 1.15 for small windows with a high speed flow.

J_f is the correction coefficient for the effects derived from leakage of partitions, including the leakage among bundle and partition and the leakage between shell and partition (A and E flows). If the wall are near to each other,

the decrease in leakage flow in comparison with cross flow increases. J_ℓ is a function of the total leakage surface ratio for every partition and for cross flow area between neighboring partitions and also the ratio of shell leakage area and partition is the same as the leakage area of partition and tube. The normal amount of J_ℓ is between 0.7 and 0.8.

J_b is the correction coefficient for the effects of bypass flows at tube bundle that is due to the looseness between the outermost tube of the shell on one hand and the channel created in the tube bundle for making tube passes on the other hand (flows F and C). For a rather small looseness between outermost shell and tube and for the shell with fixed tube sheet is $J_b \approx 0.90$.

For a shell with floating head and the ability of taking out the head and tube bundle from the shell, need a bigger looseness and $J_b \approx 0.70$. narrow pieces related to sealing can increase J_b .

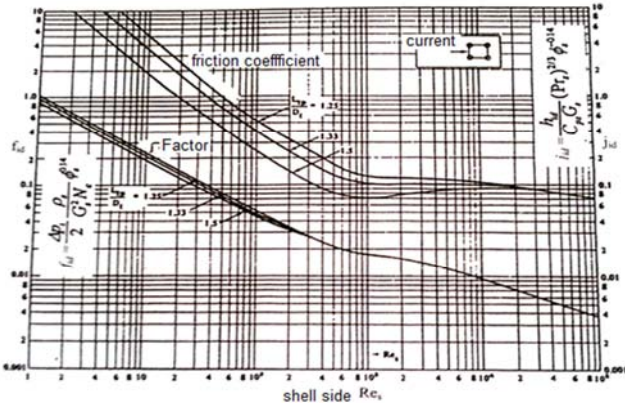


Figure 6. Coefficients of J_M and f_M , set of ideal tube for locating the periodic of 90 degree.

J_s is the correction coefficient for the changing distance of the walls at the enter and exit of the shell. Due to the more distance of the walls at the nozzle location of exit and enter of the shell and changes in the local speeds in these regions, the average of heat transfer coefficient at the shell side will change. J_s amount is usually between 0.85 and 1.

J_r coefficient is used when Reynolds number in shell side Re_s is less than 100. If $Re < 20$, this factor is completely effective and if $Re > 100$, then $J_r = 1/100$.

The mixed influence of all these coefficients for the heat exchanger of the shell and tube kind is 0.60 when the design is perfect.

2.2.2. Pressure Drop at the Shell Side

For heat exchanger of the shell and tube kind with by pass and leakage flows, the total pressure drop of the exit nozzle is calculated in the three following ways:

1. Regarding pressure drop of cross flow (in the distance of the two neighboring walls), this pressure drop in the whole shell (except at the two ends) is equal to

$$\Delta p_c = \Delta p_{b,id} (N_b - 1) R_b R_\ell \tag{21}$$

where $\Delta p_{b,id}$ is pressure drop at the tube bundle between the two internal partitions (except at the two ends of the

exchanger)

R_ℓ is the correction coefficient for the wall leakage effects (A and E flows) and it is about 0.4 to 0.5.

R_b is the correction coefficient for bypass flows (F and C flows) and it is usually about 0.5 to 0.8 and this parameter is dependent on the structure of thermal exchanger and the number of sealing strips. N_b is the number of the wall and $(N_b - 1)$ is number of the distance between internal the wall (except the two ends).

2. Pressure drop at the window is due to the leakage flow but is due to not bypass flow. The whole of pressure drop of the flow from all of window is calculated in the following way:

$$\Delta p_w = N_b \cdot \Delta p_{w,id} \cdot R_\ell \tag{22}$$

where $\Delta p_{w,id}$ is pressure drop of the flow at one ideal tube bundle at the window section.

3. Pressure drop at the exit and enter areas is affected by bypass flow but is not affected leakage flow. In addition, this pressure drop is also affected by the changing distance of the wall. Pressure drop for exit and enter areas is calculated in the following way:

$$\Delta p_e = 2 \Delta p_{b,id} \frac{N_{r,cc} + N_{r,cw}}{N_{r,cc}} R_b R_s \tag{23}$$

where $N_{r,cc}$ is the number of rows for cut tubes at the tube bundle by cross flow (the number of cut tubes rows by the any two neighboring walls) and $N_{r,cw}$ is the number of cut tubes rows by cross flow at every wall window.

R_s is the correction coefficient for exit and enter areas that due to the exit and enter nozzles have different wall distances with middle walls distances.

the total pressure drop in the thermal exchanger is

$$\Delta p_T = \Delta p_c + \Delta p_w + \Delta p_e \tag{24}$$

$$\Delta p_T = [(N_b - 1) \Delta p_{b,id} R_b + N_b \cdot \Delta p_{w,id}] R_\ell + 2 \Delta p_{b,id} \left(1 + \frac{N_{r,cw}}{N_{r,cc}} \right) R_b R_s \tag{25}$$

pressure drop in the nozzles should be calculated separately and added to the total pressure drop.

In this equation, $\Delta p_{b,id}$ is calculated in the following way:

$$\Delta p_{b,id} = 4 f_{id} \frac{G_s^2}{2 \rho_s} \left(\frac{\mu_{s,w}}{\mu_s} \right) \cdot N_{r,cc} \tag{26}$$

$\Delta p_{w,id}$ for section of the ideal window partition is calculated in the following ways:

when $Re \geq 100$

$$\Delta p_{w,id} = \frac{m_s^2 (2 + 0.6 N_{r,cw})}{2 \rho_s A_{o,cr} A_{o,w}} \tag{27}$$

and when $Re \leq 100$

$$\Delta p_{w,id} = 26 \frac{\mu_s m_s}{\sqrt{A_{o,cr} A_{o,w} \rho_s}} \left(\frac{N_{r,cw}}{P_t - d_o} + \frac{B}{D_{h,w}^2} \right) + \frac{m_s^2}{A_{o,cr} A_{o,w} \rho_s} \tag{28}$$

$D_{h,w}$ is the cross flow surface area from the windows and $A_{o,w}$ and the related correction factors

$N_{r,cc}$ the number of tube rows that is cut at the tube bundle by cross flow (the number of cut tubes rows by any two neighboring partitions) can be calculated in the following way:

$$N_{r,cc} = \frac{D_s(1 - \frac{\ell_c}{D_s})}{X_\ell} = \frac{D_s - 2\ell_c}{X_\ell} \quad (29)$$

where X_ℓ is defined in the figure 7 and tube pitch is parallel to the flow and can be obtained from table 2 and ℓ_c is the height of the wall cut.

$N_{r,cw}$ is the effective number of tube rows in the cross flow in every window and can be calculated from the following equation:

$$N_{r,cw} \approx \frac{0.8\ell_c}{X_\ell} \quad (30)$$

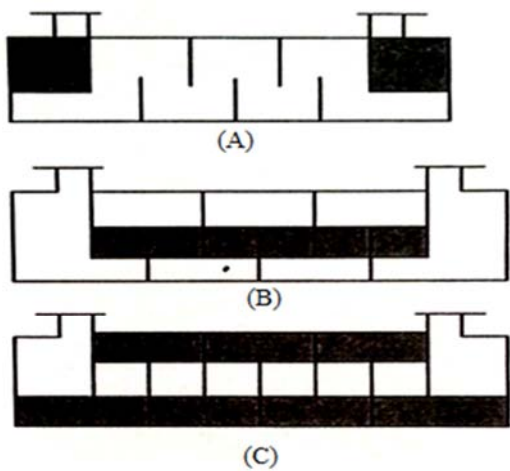


Figure 7. a) exit and enter areas, b) the distance between walls(except the two ends), c) areas with windows.

the number of walls N_b can be obtained from the following equation:

$$N_b = \frac{L - L_{b,i} - L_{b,o}}{L_{b,c}} + 1 \quad (31)$$

L is the length of thermal exchanger, and $L_{b,i}$, $L_{b,o}$, $L_{b,c}$ are the space of entrance wall, the space of exit wall and the distance between the two interval walls of heat exchanger respectively.

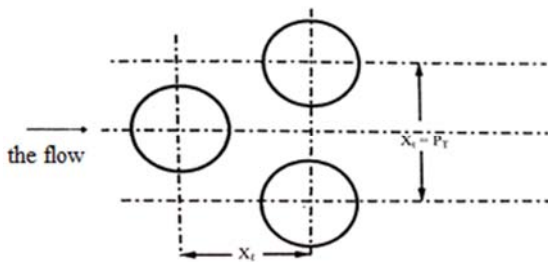


Figure 8. Tube pitches, parallel and upright with the flow. (the arrangement of equilateral triangle).

The pressure drop total at the shell side of shell and tube

heat exchanger is about 20 to 30 % of the pressure drop that is calculated ideally without taking the effects of partition leakages flow and the bypass flow of the tube bundle into account.

Table 2. Tube pitches, parallel (X_t) and upright (X_t or P_T) with the flow line.

$X_t/2$ or $P_T/2$ (in)	X_ℓ (in)	Locating	P_t X_t or Tube pitch (in)	d_o or O.D.outside diameter tube (in)
0.408	0.704	→ ◁	13/16=0.812	5/8=0.625
0.409	0.814	→ ◁	15/16=0.938	3/4=0.750
1.000	1.000	→ □	1.000	3/4=0.750
0.707	0.707	→ ◇	1.000	3/4=0.75
0.500	0.866	→ ◁	1.000	3/4=0.750
1.250	1.250	→ □	11/4=1.250	1
0.884	0.884	→ ◁	11/4=1.250	1
0.625	1.082	→ ◁	11/4=1.250	1

The studied sample of shell and tube exchanger is U shape. Its warm fluid is DM Water and is located at the shell and its cool fluid is water that is cooled in the previous process and in conversion with sea water. The aim of designing this exchanger is decreasing water temperature fluid in cooling of sulfur granulation packages. The entrance operational temperatures and pressures at both side of the shell and tube and the physical specifications of the exchanger is available. A summary of these specifications that is necessary for introducing the exchanger is provided in the tables 3 and 4.

Table 3. Thermal specifications of sulfur granulation package exchanger.

Fluid categories	Shell side	Tube side
Fluid name	Hot water (system working fluid)	Cold water
Mass flow (kg/h)	27100	13800
Temperature (In/Out) (C)	110.85 121.5	59 38
Pressure (kpa)	450	300
Speed (m/s)	0.73	1.6
Reynolds number	33328.42	25230.8
Pressure drop	16.53	10.48
Heat exchanged (KW)	337.112	

Table 4. Mechanical specifications of sulfur granulation package exchanger.

Type of exchanger (rear head/shell/stationary head)	BEU	Tube number	38
The effective area of the exchanger(m^2)	3.6	Tube pitch (mm)	18.36
Shell Outside diameter (mm)	217.5	Tube pattern	30°
Shell Inside diameter (mm)	201.5	Tube pass numbers	2
Tube inside diameter (mm)	12	Baffle type	single segmental
The thickness of the tube wall (mm)	1.5	Baffle cut	33% horizontal
Tube length (mm)	1300	Number of baffle	9

3. Geometrical Production of Exchanger

For geometrical examined in this study is the use of ASPEN B-JAC software. figures below shows a view of the shell and tube exchangers that in this the software is designed and modeled.

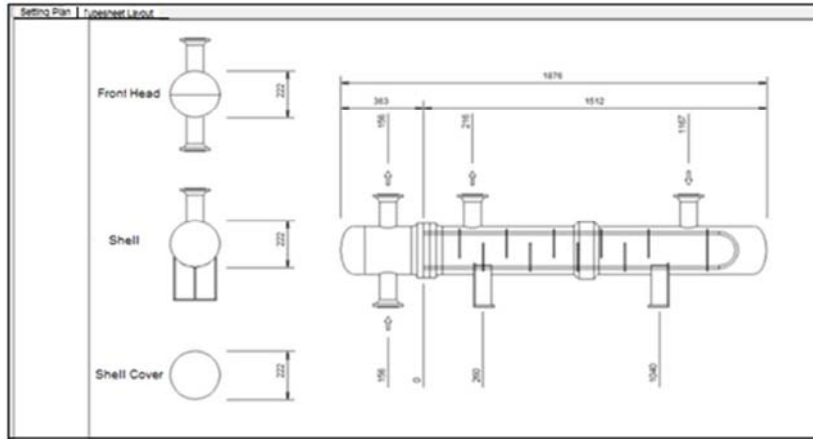


Figure 9. Designing simulated sulfur granulation package exchanger in ASPEN B-JAC software.

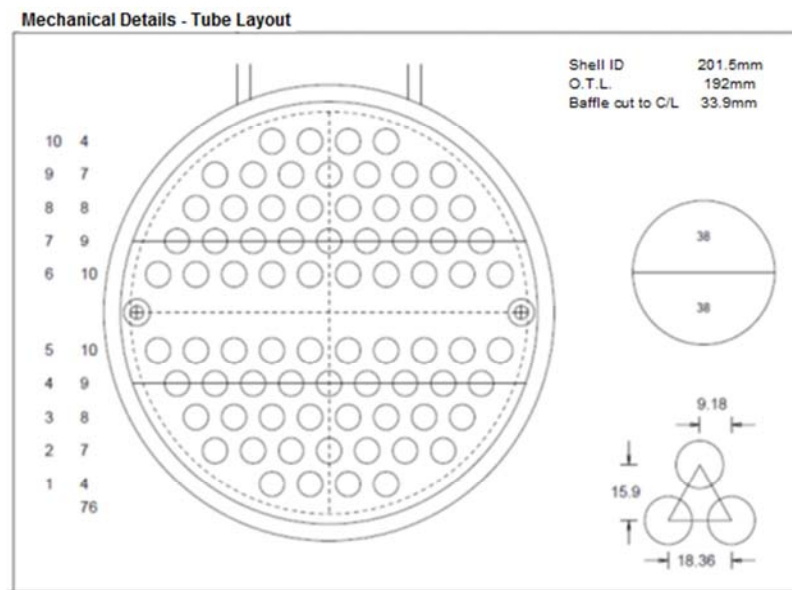


Figure 10. Arrangement of simulated sulfur granulation tube sheet exchanger in ASPEN B-JAC software.

Now, it is the time to run the program. By running the program, at first opened a new folder that shows the software status and calculation status according to figure 10.

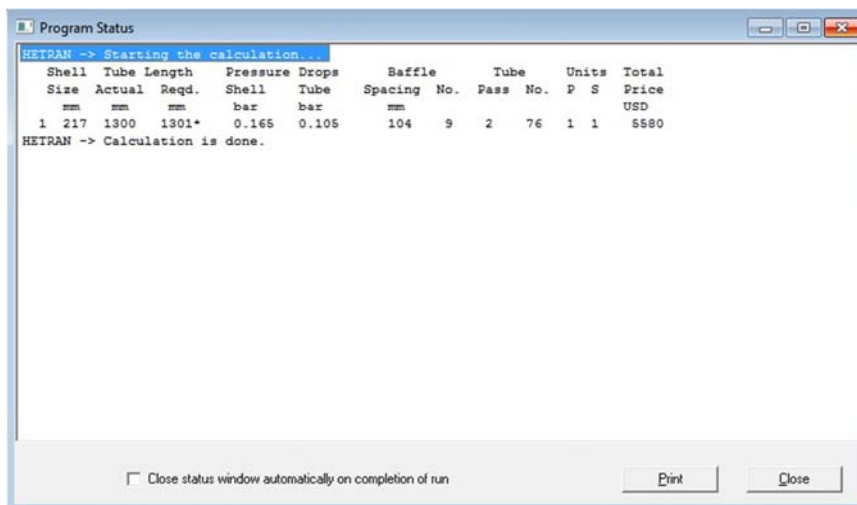


Figure 11. The software status in sulphur granulation exchanger.

4. Validating of Software with Observed Realities in the Exploitation Process

The aim of this chapter is to analyze the validity of the studies with observed realities in the exploitation process. In addition, the mechanical details of the exchanger, such as the number of tubes, arrangement and....should be in agreement with the available plans.

As it is clear in the Figure 9, the arrangement of the tubes in tube sheet of the sulfur granulation package exchanger is as same as available documents in the refinery.

Table 5. Mechanical details of sulfur granulation package exchanger, simulated in the ASPEN software.

Mechanical detail – Bundle					
Baffle type		single seg	Shell id – bundle otl clearance	mm	9.52
Inlet spacing	mm	259	Baffle hole – tube od clearance	mm	0.79
C-C spacing	mm	104	Shell id – bundle od clearance	mm	3.18
Outlet spacing	mm	120.2	Baffle od – bundle otl clearance	mm	6.35
Number of baffles		9	Pass partition lane width	mm	12.7
Supports		1	Impingement protection		None
Baffle cut	hor	33%	Sealing strips (pairs)		
Triple segmental intermediate cut		%	Outer tube limit	mm	191.98
Double/triple segmental outer cut		%	Open distance at top	mm	13.15
Baffle thickness	mm	6	Open distance at bottom	mm	13.15
Tube length	mm	1300			
Tubesheet thickness (est.)	mm	38			
Mechanical detail – Tubes					
Tube length	mm	1300	Tube o.d	mm	12
Number of tubes		76	Tube wall thickness	mm	1.5
Tube pitch	mm	18.36	Tube wall specification		ave
Tube pattern		30	Tube type		plain
Tube passes		2	Fin height	mm	
Tube pass layout		Ribbon	Fin thickness	mm	
Tubesheet thickness (est.)	mm	38	Fin density	#/m	
Tube-tubesheet joint		groove/expand	Area ratio Ao/Ai		1.33
Pass partition lane width	mm	12.7	Twisted tape insert width	mm	
Deviation in tubes/pass		%	Twist ratio		

The most important point in validating of simulated exchanger in the ASPEN software is adjusting the external temperature of cool and warm fluid of exchanger with the reality.

As it is clear from Table 6 for sulfur granulation package exchanger, the external temperature of the exchanger is 110 for warm fluid and 59 for cool fluid. these numbers are near to reality. the other point is the amount of exchanged heat in the exchanger that is in accordance with reality for the

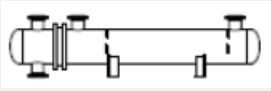
amount 337 KW.

Now, after being sure about the precise of exchanger simulation results in the software, can follow necessary actions for optimizing these exchangers in the following chapter. The process is in the following way: Changed, parameters that are flexible in the tube bundle of mentioned exchanger and analyzing their effects on the heat transfer rate and exchanger efficiency.

Table 6. Technical information sheet of simulated sulphur granulation exchanger in aspen B-JAC software.

Heat Exchanger Specification Sheet										
1	Company: South Pars Gas Complex (SPGC)									
2	Location: Assaluyeh									
3	Service of unit: Sulphur			Our Reference:						
4	Item No: 144-E-103			Your Reference:						
5	Date:	Rev No:	Job No:							
6	Size	201---1300	mm	Type	BEU	hor	Connected in	1 parallel	1 series	
7	Surf/unit(eff.)	3.6	m ²	Shells/unit	1		Surf/shell(eff.)	3.6	m ²	
8	PERFORMANCE OF UNIT									
9	Fluid allocation			Shell Side			Tube Side			
10	Fluid name			water_hot			Water_cold			
11	Fluid quantity, Total			7.5278			3.8333			
12	Vapor (In/Out)			kg/s						
13	Liquid			kg/s			7.5278 7.5278 3.8333 3.8333			

14	Noncondensable	kg/s								
15										
16	Temperature (In/Out)	°C	121.5		110.85		38		59	
17	Dew / Bubble point	°C								
18	Density	kg/m ³	941.52		950.28		995.1		986.04	
19	Viscosity	mPa s	0.239		0.26		0.678		0.481	
20	Molecular wt, Vap									
21	Molecular wt, NC									
22	Specific heat	k J/(kg K)	4.21		4.202		4.188		4.185	
23	Thermal conductivity	W/(m K)	0.687		0.683		0.617		0.642	
24	Latent heatk	J/kg								
25	Pressure	bar	4.5				3			
26	Velocity	m/s	0.73				1.6			
27	Pressure drop, allow./calc.	bar	0.68948		0.17933		0.68948		0.11852	
28	Fouling resist. (min)	m ² K/W	0.0002				0.0002			
29	Heat exchanged	337112	W		MTD corrected		66.98		°C	
30	Transfer rate, Service	1391.9	Dirty	1392	Clean	3972.6			W/(m ² K)	
31	CONSTRUCTION OF ONE SHELL							Sketch		
32			Shell Side		Tube Side					
33	Design/Test pressure	bar	5.17107/	/Code	5.17107/	/Code				
34	Design temperature	°C	160		93.33					
35	Number passes per shell		1		2					
36	Corrosion allowance	mm	1.59		1.59					
37	Connections	In	76.2		76.2/150 ANSI					
38	Size/rating	Out	76.2/150 ANSI		76.2/150 ANSI					
39		mm/	Intermediate		/150 ANSI					
40	Tube No. 38Us	OD 12	Tks-avg	1.5	mm	Length 1300	mm	Pitch 18.36	mm	
41	Tube Type plain		Material SA-106 Gr B					Tube pattern 30		
42	Shell SA-106 Gr B	ID 2011.5	OD 217.5		mm	Shell cover		SA-106 Gr B		
43	Channel or bonnet	CS				Channel cover				
44	Tubesheet-stationary	SA-516 Gr 70				Tubesheet-floating				
45	Floating head cover					Impingement protection	None			
46	Baffle-crossing	SA-106 Gr B	Type single seg	Cut(%d)	33	hor	Spacing: c/c 104		mm	
47	Baffle-Long		Seal type				Inlet	259	mm	
48	Supports-tube	U-bend	Type							
49	Bypass seal		Tube-tubesheet joint			groove/expand				
50	Expansion joint		Type							
51	RhoV2-Inlet nozzle	2897	Bundle entrance	352		Bundle exit	1621		kg/(m s ²)	
52	Gaskets – Shell side		Tube Side							
53	Floating head									
54	Code requirements	ASME	Code Sec VIII Div 1			TEMA class	B			
55	Weight/Shell	201.3	Filled with water	245.6		Bundle	50.8		kg	
56	Remarks									



5. Analyzing Effective Factors on the Efficiency of Sulfur Granulation Package Exchanger

5.1. Analyzing the Number of Tube Passes

In this section, will change the passes of the mentioned exchanger at the tube side. case study (sample of study) has two tube passes. Change in the passes at the tube side will affect thermal rate, pressure drop at the shell and tube side and the speed of the flow at the tube side. It should be mentioned that will decrease the number of tubes to 34 in 4-passing state that can be placed in the mentioned shell diameter. So it is not feasible to analyze more than 4 passes due to its shell small diameter. Because decrease in the thermal exchange rate due to decrease in the number of tubes and heat transfer effective level is high.

As figure 12 shows, the thermal rate of 2 passes state is more than other states. while expected that with an increase in passes, two fluids have more opportunity for sharing heat

and in line with that heat rate in the four state pass will be more than that of two state pass. But it should be noted that it was our analysis that was not true, not the results of the software. As it was stated, it had to decreased the number of tubes to 34 in 4 state pass that lead to a decrease in heat transfer level and heat rate.

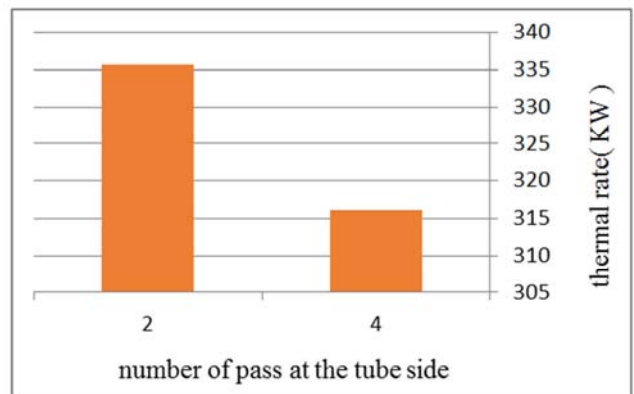


Figure 12. Thermal rate according to the passes at the tube side.

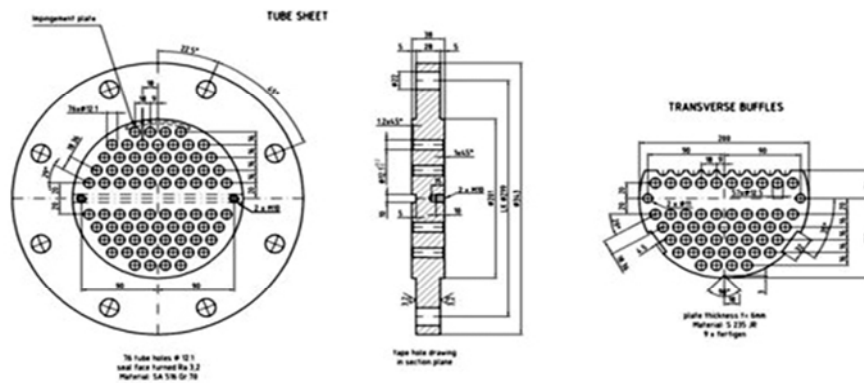


Figure 13. The view from tube sheet and the baffle of sulphur granulation exchanger.

Regarding the Figure 14, can see that pressure drop at the shell side in state of two pass is more than that in other states as it is in the heat rate. With the same reason, with a decrease in the number of tubes, the obstacles around the flow will decrease that lead to a decrease in pressure.

Of course, An increase at the tube passes will lead to an increase in the pressure drop at the shell side, but as it is observable in the four state pass, this increase is less than pressure drop at due to a decrease in the number of tubes.

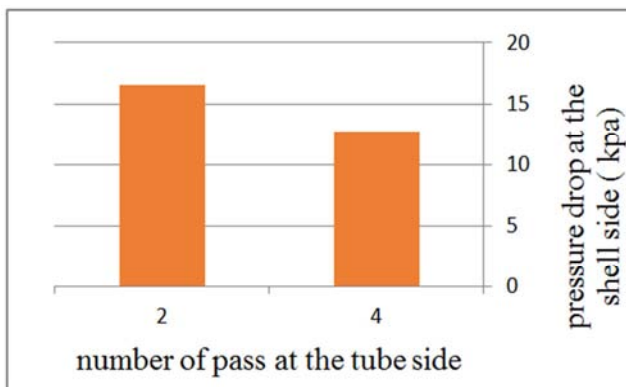


Figure 14. Pressure drop at the shell side according to the passes at the tube side.

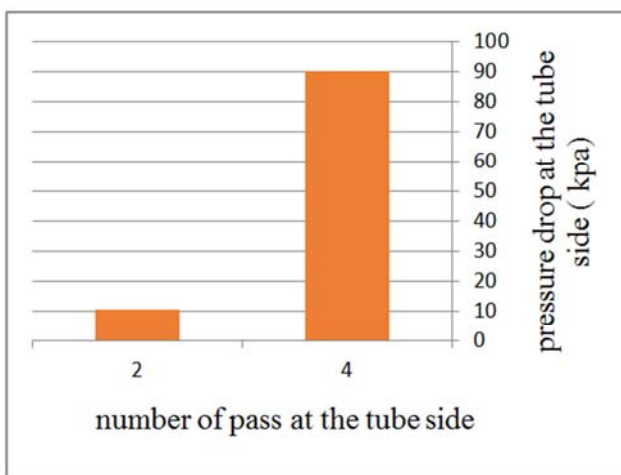


Figure 15. Pressure drop at the tube side according to the passes at the tube side.

Figure 15, indicates that pressure drop at the tube side in four state pass is more than that in other states. an increase in the number of passes will lead to a decrease in the number of available tubes. So, assuming that the mass is instant, flow speed at the tubes will increase. Although this increase of speed will increase, movement coefficient and decrease scaling, but it will lead to increase of pressure drop.

5.2. Tube Arrangement Analysis

Table 7 shows the maximum number of embedded tube in 4 arrangement models including the following shapes: triangle (30), rotated triangle (60), square (90) and rotated square (45). In triangle and rotated triangle arrangement, there are more tubes. In addition, triangle arrangement has a higher turbulence and higher heat transfer coefficient and pressure drop, but cannot clean the tubes effectively due to the inappropriate distance for crossing the cleaner.

Table 7. The maximum number of placed pipes in the sulfur granulation exchanger shell according to the tubes pattern.

Tube pattern	30	45	60	90
Number of tube	38	28	34	32

In table 7 shows the effect of tube arrangement in the exchanged heat. As it is expected, the number of tubes and heat transfer level has direct relation with thermal exchange rate.

In figure 16 shows, Thermal rate based on tubes pattern. as was expected, number of tubes and heat transfer surface has directly proportional with heat exchange rate.

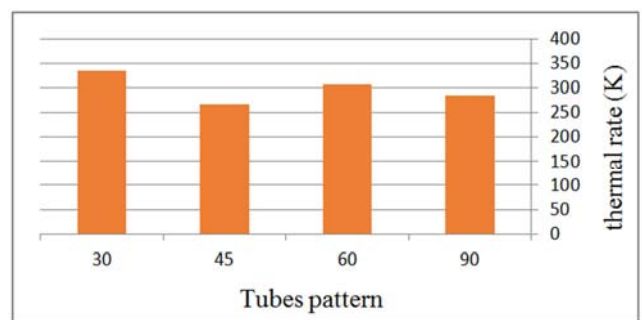


Figure 16. Thermal rate according tubes pattern.

Based on figure 17, it can be seen that in every arrangement, when the tubes pattern is dense, can have more pressure drop, apart from the increase in the number of tubes in the fixed diameter of the shell. As you see, the higher number of tubes with 90 degree arrangement does not cause its pressure drop to be more than that of 45 degrees. In other words, the effect of tube pattern on pressure drop in 45 degree model is more than the effect of having more tubes in 90 degrees.

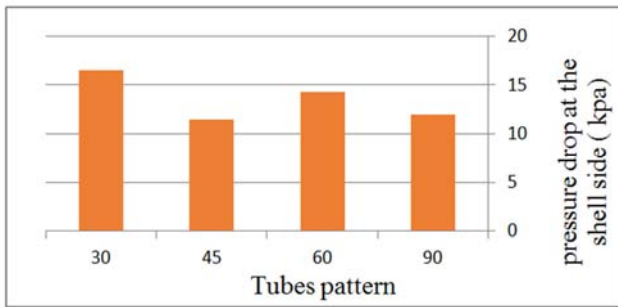


Figure 17. Pressure drop at the shell side according to tubes pattern.

5.3. Analyzing decrease in tubes pitch

The important point in analyzing decrease in pitch of tubes of shell and tube exchanger is that, can do the work practically because of the limitation in their connection to the tube sheet and decrease in the bending radius of the tubes. According to the available documents, it can decrease the tube pitch, up to 1.25 of tube outer diameter and this amount should increase for the cases in which tube connection to the tube sheet is of welding kind. Table 8 shows the maximum number of embedded tubes with a decrease in the tubes pitch.

Table 8. The maximum number of embedded tubes in the sulfur granulation exchanger according to the tube pitch.

Tube pitch (mm)	16.5	17.5	18.36
Number of tube	47	40	38

In figure 18, the effect of tubes pitch on exchanged heat rate be shown. As it is expected due to increase in the number of tubes and increase in the heat transfer level, the exchanged heat rate has increased.

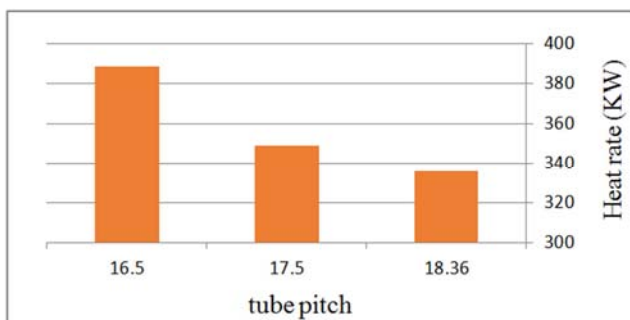


Figure 18. Heat rate based on tube pitch.

In figure 19 and 20, pressure drop due to the tubes pitch decrease at the shell and tube side of exchanger is analyzed

and as it is predictable, pressure drop process at the shell side is increasing due to the increase in the number of tubes and it will increase and at the tube side because that the fluid will be able to pass a lot of tubes, will decrease.

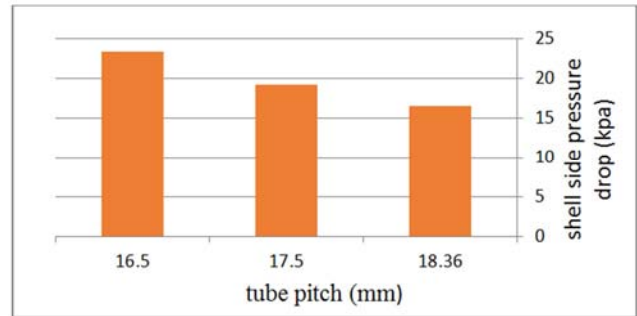


Figure 19. Pressure drop at the shell side according to the tube pitch.

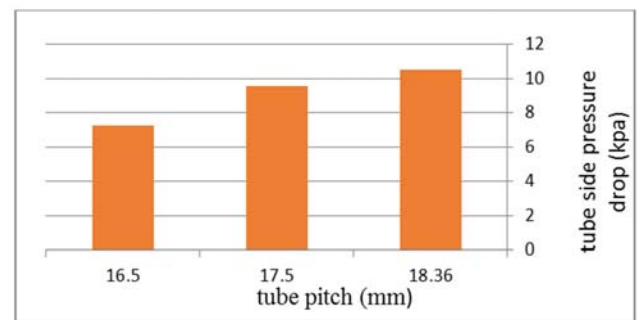


Figure 20. Pressure drop at the tube side according to the tube pitch.

6. Offers

It is suggested that take be considered optimizing the other exchangers for refinery due to the large number of exchanger in refinery processes and the necessity of decreasing energy consumption. The important point is that need exact data of the fluids of this process so that can optimize and simulate them with the help of ASPEN B-JAC software. Usually, the fluid in the refinery exchangers consists of several hydrocarbons with different thermal coefficients and evaporation temperatures and different physical specifications that make simulation difficult.

7. Conclusion

In this thesis, one exchanger of south pars refineries, phases 9 and 10 was analyzed. The exchanger was sulfur granulation package with the job of adjusting the cooling fluid temperature of these packages. The importance of this exchanger is that not controlling it in an appropriate way can distort in the process of sulfur granulation and the results will be to sulfur burning and damage to the eco-system.

In this study one exchanger of south pars refineries, phases 9 and 10 were investigated. The first exchanger was in the sulfur granulation package which has the function of regulating the temperature of the cooling systems. The importance of these exchanger is due to the fact that the inability in controlling it properly impairs the process of

sulfur granulation.

With a change in the design of the mentioned thermal exchanger and having proposals according to the table 9 that makes thermal transfer of the two fluids easier, can decrease the necessary energy for cooling this fluid and reduced the cost of pumping the sea water.

The manner in which the choices are made is in this way that consider two pass for optimized exchanger to the permitted pressure drop at the tube side. Arranging the pipes tubes change to 30 degrees, because can use more tubes. And also can decrease the tube pitch from 18.36 up to 16.5, which causes the placement of more tubes in the exchanger and increases the extent of exchanged heat.

Table 9, shows the comparison of the suggested exchanger with the main model exchanger.

Table 9. The comparison of the suggested exchanger for sulfur granulation package with the main model exchanger.

	Main model exchanger	Suggested exchanger	Change percent
Thermal rate	1378.762	1496.5	8.5
Pressure decrease at the shell	1.765	1.505	-14.73
Pressure drop at the tube	12.26	18.201	48.46
Maximum number of tubes	56	109	94.64
Final production cost	18340	19100	4.14

Nomenclature

Latin symbols

T	fluid temperature (K)
Q	conservative variable vector
he	introduced the total energy
M_t	Mach of turbulent flow
c_p	specific heat ($\text{Jkg}^{-1}\text{k}^{-1}$)
Δp	overall pressure drop (Pa)
DT	logarithmic mean temperature difference (K)
h_o	heat transfer coefficient in the shell side
D_e	the diameter of the shell
G_s	mass speed of shell side

Greek symbols

μ	dynamic viscosity ($\text{kgm}^{-1}\text{s}^{-1}$)
μ_t	turbulent dynamic viscosity ($\text{kgm}^{-1}\text{s}^{-1}$)
ν_t	turbulent kinematic viscosity (m^2s^{-1})
ν	kinematic viscosity (m^2s^{-1})
ε	dissipation rate of turbulent (m^2s^{-3})
ρ	density (kg m^{-3})
a	speed of sound
σ_k	Prandtl number of k
σ_ε	Prandtl number of ε
Ω	rotation absolute value
λ	thermal conductivity ($\text{Wm}^{-1}\text{k}^{-1}$)

Subscripts

In	inlet
Out	outlet
s	shell side
t	tube side

References

- [1] American Society of Mechanical Engineers, (2013), "ASME Boiler and Pressure Vessel Code-An International Code", Section VIII, Division 3, Alternative Rules for Construction of High Pressure Vessels, New York.
- [2] Bell, K. J. (1981), *Preliminary design of shell and tube heat exchangers. In Heat Exchangers: Thermal-Hydraulic Fundamentals and Design*, S. Kakac, A. E. Bergles, and F. Mayinger (Eds.), Taylor & Francis, Washington D.C., pp. 559-579.
- [3] Bell, K. J., (1981), *Delaware method for shell-side design. In heat exchangers: Thermal-hydraulic fundamentals and design*, S. Kakac, A. E. Bergles, and E. Mayinger (Eds.), pp. 581-618. Taylor & Francis, Washington D.C.
- [4] Fraas, A. P., (1989), *Heat Exchanger Design*, Wiley, New York.
- [5] Gaddis, Daniel, (2007), "Standards of the Tubular Exchanger Manufacturers Association", Tubular Exchanger Manufacturers Association [TEMA], Inc., 9th Edition, New York.
- [6] Hewitt, G. F., Shires, G. L., and Bott, T. R., (1994), *Process Heat Transfer*, CRC Press, Boca Raton, FL.
- [7] Sadik Kakac and Hongtan Liu., (2002), *Heat Exchanger selection: rating and thermal design book*, (2nd ed.). CRC Press.
- [8] Saunders, E. A., (1988), *Heat Exchanges: Selection, Design and Construction*, New York: Longman Scientific and Technical.
- [9] Taborek, J., (1983), *Shell-and-Tube Heat Exchanger. In Heat Exchanger Design Handbook*, E. U. Schlunder (Ed), Section, 3.3. Hemisphere, New York.
- [10] Tinker, T., (1951), *Shell-side Characteristics of Shell-and-Tube Heat Exchanger. General Discussion on Heat Transfer*, pp. 97-116. Institute Mechanical Engineering and ASME, New York, London.
- [11] Holman J. P., 2002. *Heat Transfer*, 9th Edition, McGraw-Hill.
- [12] Hossain, S. N., and Bari, S., (2011), "Effect of different working fluids on shell and tube heat exchanger to recover heat from exhaust of an automotive diesel engine". World Renewable Energy Congress.
- [13] Dizaji H. S., Jafarmadar S., Hashemian M., 2015. *The effect of flow, thermodynamic and geometrical characteristics on exergy loss in shell and coiled tube heat exchangers*, *Energy conversion and management*, Vol. 91, PP. 678-684.
- [14] Gao B., Bi Q., Nie Z. and Wu J., 2015. *Experimental study of effects of baffle helix angle on shell-side performance of shell-and-tube heat exchangers with discontinuous helical baffles*. *Experimental thermal and fluid Science*, Vol. 68, PP. 48-57.
- [15] Yang J. F., Zeng M., Wang Q. W., 2015. *Numerical investigation on combined single shell and tube heat exchanger with two-layer continuous helical baffles*, *International Journal of Heat and Mass transfer*, Vol. 84, PP 103-113.